DETERMINING STRAIN RATE DEPENDENCE OF HUMAN BODY SOFT TISSUES USING A SPLIT HOPKINSON PRESSURE BAR

A. Chawla, S. Mukherjee, R. Marathe, B. Karthikeyan
Indian Institute of Technology, Delhi
R. Malhotra
All India Institute of Medical Sciences, Delhi

ABSTRACT

Crash simulations with Finite Element human body models would be better predictors of injury than with dummy models. During dynamic loading, human body soft tissues are exposed to varying strain rates. To characterize them, the conventional Split Hopkinson Pressure Bar (SHPB) is modified in order to test soft tissues. Experimentally determined engineering stress vs engineering strain curves for erector spinae, hamstring and gluteus max muscles are reported in the strain rate range of from 250/s to 1000/s. The loading curves exhibit multi linear behavior with increasing strain rate shifting the transition points between the slopes.

Keywords: Human Body, Soft Tissue, Split Hopkinson Pressure Bar, Rate Dependency, Materials.

CRASH SIMULATIONS WITH accurate Finite Element human body models would be better predictors of injury than with dummy models. During dynamic loading as in crash situations, human body soft tissues are exposed to varying strain rates. It is to be ascertained if the strain rate dependence of soft tissues is significant enough to modify the impact response. If so, these responses need to be characterized to be reproducible in simulation. To characterize strain rate dependence of materials, one established experimental procedure used has been the Split Hopkins on Pressure Bar (SHPB). For conventional materials, the SHPB uses metallic rods with a impedance close to that of the material to be tested. The SHPB setup for these materials typically uses long rods and the whole setup is a few meters long. These setups also target strain rates of up to10^6/s. For pedestrian impacts the required strain rate in muscular soft tissues of the lower leg, estimated on the basis of a typical duration of 1 ms for the loading phase during impact, would be of the order of 10^3/s. The SHPB has been successfully modified in the present work in order to test Human Body soft tissues. Sligtenhorst et al. (2005) have also developed an SHPB for soft tissues and have tested bovine tissues using the same. Cheng et al., (1998) have discussed how attenuation factors can be calculated using spectral analysis in a visco-elastic SHPB. In the present study we have developed the polymeric SHPB for testing human soft tissues. We estimate the attenuation using experimental techniques described in Bacon (1998). The target material for testing is human soft tissue left over from surgical procedures, also called ‘surgical scrap’. The setup is hence designed on the basis that the size of the tissue sample available is very small, often giving only 2-3 specimen 10-15mm square in cross-section.. Secondly, the eventual target location of the setup is in operation theaters for testing within half an hour from removal before the measurable characteristics of the tissue change appreciably from in-vivo conditions.

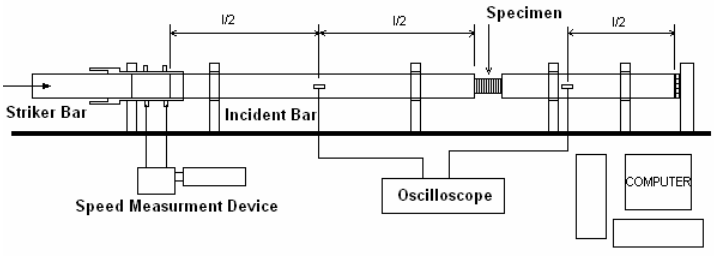

Fig. 1- Schematic of the SHPB

BASICS OF THE SHPB

The SHPB, schematically shown in Fig. 1 is one of the most widely accepted tests for characterizing materials at large strain rates. A striker impacts the incident bar setting up a traveling longitudinal strain wave which is tracked by strain gauging. A specimen is introduced in between the incident bar and reflecting bar. The stiffness characteristics of the specimen attenuate the wave transmission, modifying the pulse transmitted to the reflecting bar and reflected back from the interface to the incident bar.

Typically, the incident and reflecting bar are selected in such a manner that the impedance of the bar is close to the impedance of the material to be tested. In order to achieve this, the bars for testing soft tissues are made of poly methyl-methacrylate (acrylic) (Chen, 1999; Sawas, 1998; Zhao, 1997; Yunoshey, 2001);.which has significantly higher material damping than metal bars used in conventional setups. In these bars attenuation and dispersion of the wave is inevitable as the wave propagates through the polymeric material. We characterize the attenuation and dispersion by an experimental procedure established by Bacon and Brun (2000) and then reconstruct the pulse at the bar-specimen interface (Bacon and Brun, 2000; Zhao et al., 1997).

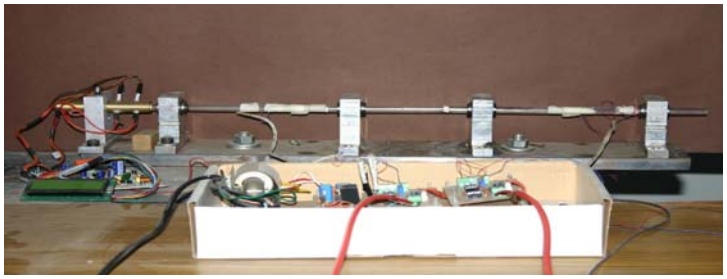

Fig. 2- Experimental setup with instrumentation

CONVENTIONAL SPLIT HOPKINSON PRESSURE BAR ANALYSIS For an SHPB with a conventional (elastic) material it is assumed that the stress acting on each cross-sectional area of the bar is uniform, the bar is stressed within the elastic limit, attenuation and dispersion are negligible and that the specimen remains in equilibrium throughout the test. With these assumptions the equilibrium of an element of length δx (Fig. 3) gives the following relation:

$$\frac{\partial^2 u}{\partial t^2} = c_o^2 \frac{\partial^2 u}{\partial x^2}, \text{ where } c_o = \sqrt{\frac{E}{\rho}}$$

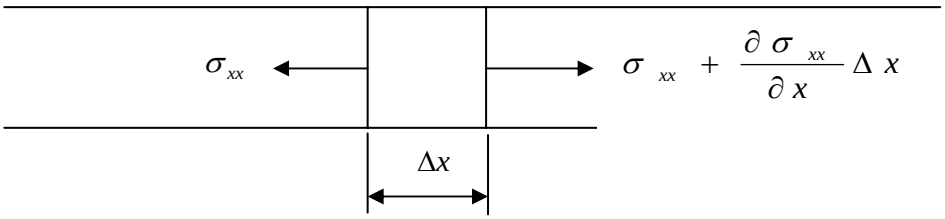

Fig. 3- Schematic of an element in a SHPB

The solution of this equation may be written as:

$u = f(c_o t - x) + F(c_o t + x)$, Where f and F are arbitrary functions and depend on the initial conditions. Considering the wave traveling in the direction of decreasing *x*,

$$u = f(c_o t + x)$$

From this, $\frac{\partial u}{\partial t} = c_0 \frac{\partial u}{\partial x}$ and since $\frac{\partial u}{\partial x} = \frac{\sigma_{xx}}{E}$, we get

$$\sigma_{xx} = \left(\frac{E}{c_o}\right)\frac{\partial u}{\partial t} = \rho c_o \frac{\partial u}{\partial t}$$

This shows that there is a linear relationship between stress at any point and particle velocity. The quantity ρc_o is called as characteristic impedance and is defined as the ratio of force to particle velocity (Graff 1991).

Considering the wave traveling in both direction of '*x*' after subsequent reflection from the end of the bars, the particle displacement in the striker and incident bars, can be written as:

$$u_s(x,t) = f_s(x - c_o t) + F_s(c_o t + x)$$

$$u_i(x,t) = f_i(x - c_o t) + F_i(c_o t + x)$$

Differentiating and using the initial conditions and known bar properties in this case, it can be shown that (Graff, 1991)

$$f_s' = -F_s' = -\frac{V_s}{2c_o} \text{ and } f_i' = F_i' = 0$$

Thus, at the instant of impact, the constant velocity-no stress situation existing in the striker bar is represented by two rectangular wave shapes, as shown in Fig. 4 at time, *t=0*.

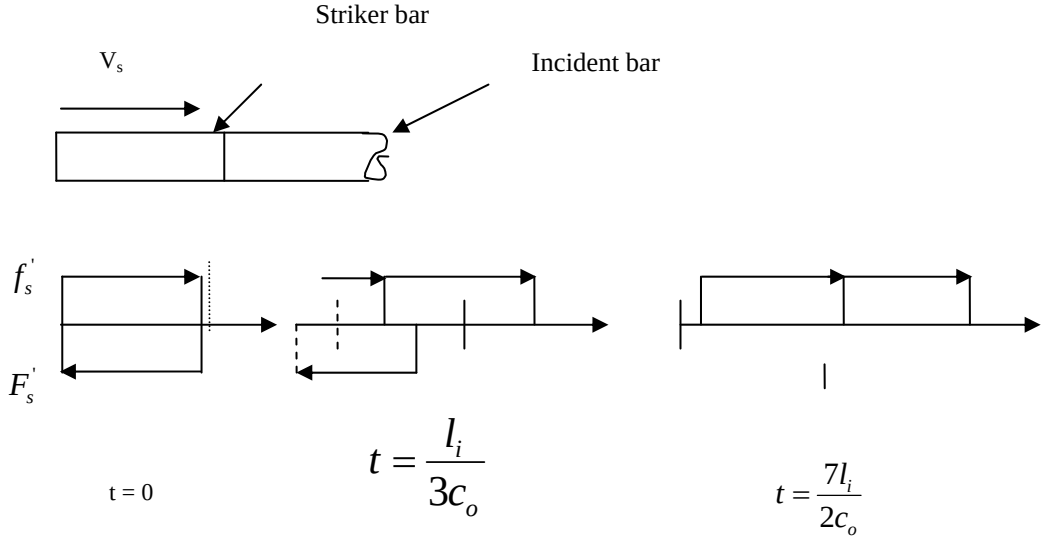

Fig. 4- Several stages of wave propagation in the collinear impact of bars (Graff, 1991)

From Fig. 4 it can seen that the length of the pulse, l_p is $2l_s$ and the duration of the pulse, T is $\frac{2l_s}{c_o}$.

The average stress in the specimen can be related to the forces exerted on each face of the specimen. Fig. 5 shows a cylindrical specimen subjected to forces exerted by the input and output bars.

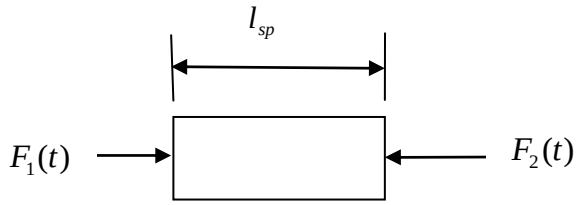

Fig. 5- Schematic of a cylindrical specimen

The forces at the end of the pressure bars may be expressed in terms of the incident and reflected pressure bar strains and the average stress can be calculated as

$$\sigma_{avg}(t) = \frac{Ed_{bar}^2}{2d_{sp}^2}\left[\varepsilon_i(t) + \varepsilon_r(t) + \varepsilon_t(t)\right]$$

where d_{bar}, and d_{sp} are the diameters of the bar and the specimen respectively and the subscripts *i*, *r* and *t* refer to the incident, reflected and transmitted pulses.

Thus the average stress in the specimen can be calculated by measuring $\varepsilon_i(t)$, $\varepsilon_r(t)$ and $\varepsilon_t(t)$ using strain gauges mounted on the transmitter bar. The strain rate is defined as strain divided by time over which the straining occurs. Therefore, strain rate in deforming specimen is given by (ASM Hand Book, 1998):

$$\frac{\partial\varepsilon}{\partial t} = \frac{v_1 - v_2}{l_{sp}} = \frac{c_o}{l_{sp}}\left[\varepsilon_i(t) - \varepsilon_r(t) - \varepsilon_t(t)\right]$$

The total strain can be calculated by integrating the above equation over the duration of the pulse.

CORRECTION WHILE USING POLYMERIC BARS IN SHPB The analysis given above is for the Conventional Split Hopkinson Pressure bar i.e. SHPB having metallic bars. In an SHPB it is important that the impedance of the bar should be of the same order as that of the specimen being tested. Therefore, in the present study polymeric bars are used. These bars are visco-elastic in nature. When polymeric or viscoelastic bars are used the wave attenuates and disperses in the medium, hence the strain measured by the strain gauges (at the mid location of the bar) is not the same as the strain at the specimen interface. To account for this, attenuation and dispersion correction has to be done. To find the attenuation and the propagation coefficient we use the procedure developed by Bacon (1998). In the procedure the incident bar is kept in a free-free condition (that is, free at both ends in the direction of impact) and is impacted with the help of the striker bar. If the bar was made of an elastic material, the incident and the reflected pulse would be equal in magnitude and would not be dispersed. For a visco-elastic rod the reflected pulse must be reconstructed using the attenuation and dispersion coefficients. The correction coefficients can also be calculated by analytical method provided the exact material properties of the bar are known. However, Bacon and Brunn (2000), present an experimental procedure to measure the attenuation and dispersion in a visco-elastic bar. They impact a free bar with impactors of different sizes and get the attenuation and dispersion at different frequencies. In the current study, we use this experimental method to get the attenuation and the dispersion.

EXPERIMENTAL SETUP

The overall dimensions of the test rig shown in Fig. 2 are 0.5mx0.015mx0.025m. This includes the launcher as well as the velocity measuring system. The bars for the setup are made of 10 mm diameter poly methyl-methacrylate (acrylic). The length of incident as well as the transmitted bar is 0.25 m. The striker bar is of length 0.1 m. For measuring the velocity of the striker bar, an infra red sensor and receiver system is used. The sensors are controlled by an in house developed microprocessor circuit. Two sets of sensor and receiver are separated by a distance of 20mm. The readout stores the time interval between the intercepts of the two sensors as the striker passes by. The incident velocity of the striker is determined from the flight time and the distance. The strain gauges used in the setup are of the foil type with active length 1.5mm and resistance of 120 ohms. The strain gauge forms a part of a Wheatstone bridge whose output is conditioned and amplified. Data acquisition was done with the help of a storage oscilloscope and post processed with the help of a LABVIEW program. Due to the small dimension of the experimental setup, the propagation losses are minimized. The striker bar is launched from a spring loaded gun. A typical response curve is shown in Fig. 6 below. The pulse is typically of 0.5 ms duration. We found that proper mounting of the specimen is very important and any initial pre-compression of the sample results in loss of the low-strain region of the curve.

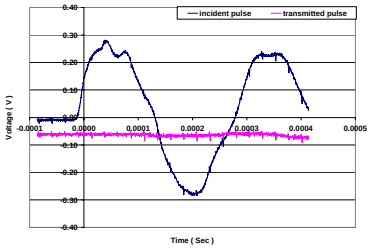

Fig. 6- Typical pulse obtained from strain gauges

SAMPLE PREPERATION

The tissues to be used for testing are obtained from the leftover of surgical procedures. Hence the size of the tissue samples available for the testing is expected to be irregular in shape and small. Also it should be possible to test the same muscle at varying strain rates to characterize the strain rate dependency of the tissue. The average size of the sample obtained from All India Institute of Medical Sciences (AIIMS) is 4cm x 2cm and a typical sample is shown in Fig. 7. Typically six to eight specimens as shown in Fig. 8 were prepared from each sample. When samples have their major dimension perpendicular to the fiber, the shapes become irregular when thawed. More regular specimen geometries are obtained when one of the major dimensions is along the fiber. We were interested in testing tissues perpendicular to the fiber direction as most automotive related impacts involve similar loading.

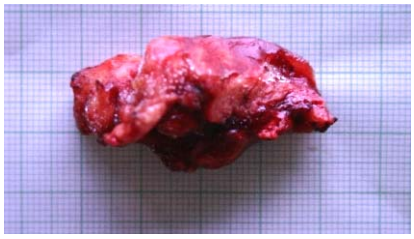

Fig. 7 Complete sample as obtained from AIIMS

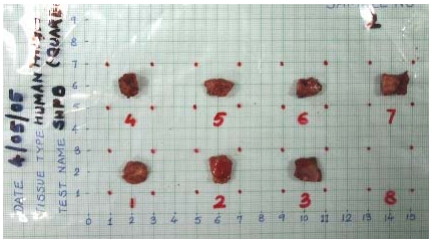

Fig. 8 Specimens prepared in laboratory for testing

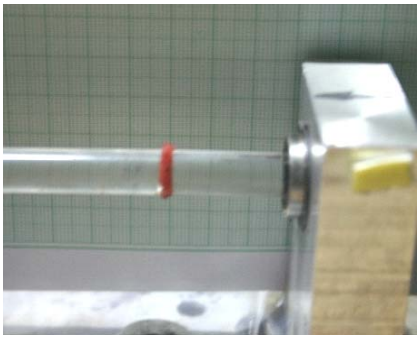

Fig. 9- Specimen after mounting

While our target is to do tests on fresh (with few hours of extraction) samples, at this stage of establishing the procedure the tests reported here have been done on frozen tissues. Leftovers obtained from AIIMS are stored at -70^{o} C. Special care was taken while handling such specimen so as not to prestrain the specimen and to retain its moisture content. Blood splatter was observed on impact, indicating that significant moisture content was retained in the sample. The frozen samples were cut with surgical blades into blocks having average size of 10x10mm. The thickness was kept to an order of 2-8 mm as Sligtenhorst et al. (2005) reports that thicker specimen tend to have non-uniform axial loading. The prepared samples were again placed in the freezer and later thawed to 20^{o} C prior to testing. The average thawing time for the tissues was 15 minutes. No preconditioning was done on the tissues. However if any blood clot was visible on the surface, it was removed before testing. The test ID nomenclature used for reporting here is *H'x'*-T '*x*' where '*H*' indicates human sample while suffix *x* will indicate the group number and '*Tx*' indicates the test number. The various tissues tested are listed in Table 1.

For sample H3, 3 tests were first done at one strain rate to demonstrate the repeatability of the setup. One more test was then done at a higher strain rate. From the other samples (H1 and H2), nine specimen were typically targeted for testing at three different strain rates with upto three specimens at each strain rate. This was done to establish the repeatability of the data and also to establish the strain rate dependency of the soft tissue for the anatomical region from which the sample was taken. Some of these specimen did not yield correct data because of experimental errors like failure in data acquisition, specimen slippage and projectile launcher malfunction. Tables 1 and 2 show the list of successful tests.

Table 1. Tissue obtained for testing and number of samples prepared from the tissue

Test ID	Anatomical Region	Number of samples tested
H1	Erector spine (male 22 yr, 60 kg)	6
H2	Hamstring(female 65 yr, 56kg)	6
H3	Gluteus Max (male 41 yr, 65 kg)	4

Table 2. Overview of the tests conducted

Subject ID-Test ID	Specimen Height (mm)	Initial velocity (m/s)	Strain rate (/s)
H1-T1	8.0	4.76	248
H1-T2	7.0	4.76	300
H1-T3	5.0	5.128	400
H1-T4	7.0	5.40	294
H1-T5	6.5	5.12	270
H1-T6	7.0	5.71	295
H2-T1	2.5	5.12	850
H2-T2	3.0	5.26	737
H2-T4	5.0	4.76	875
H2-T5	3.5	6.06	853
H2-T6	3.0	4.87	437
H2-T7	3.0	5.12	796
H3-T1	4.0	5.88	556
H3-T2	2.0	5.12	1001
H3-T3	2.5	3.8	550
H3-T4	5.0	5.71	558

RESULTS

Tests were performed on samples of the Para spinal erector spinae muscle, the hamstring and the gluteus max.

Table 2 gives the list of tests conducted along with the strain rates obtained. While six specimen each were successfully tested from the H1 and H2 samples, only four tests were successful from the H3 sample. The maximum strain as well as strain rate that can be achieved depends upon the specimen thickness. Depending on the sample thickness, three different strain rates were targeted for the samples H1 and H2. The strain rate for sample H1 was in the range of 250 – 400 while for H2 it was in the range of 430 to 850. For three of the specimen in H3 the strain rate was targeted at 550 to check the repeatability of the procedure. The loading direction in all cases was perpendicular to the fiber orientation.

The stress-strain relation with varying strain rate for H1 is shown in Fig. 10. For the H1 sample, the typical thawing time for the samples was 35 minutes since the specimen are thicker. Of the six samples tested, target strain rates were 400/s , 300/s and 250/s. Referring to

Table 2, three clusters were obtained at average values 400/s, 296/s (three samples) and 259/s (two samples) were obtained. The clusters are shown in Fig. 10 with the average values as the curves and bars representing the bounds. The maximum engineering strain that was achieved at a strain rate of

400/s was 0.17 and the maximum stress was 0.15 MPa. The results indicate significant strain rate dependence of the loading curve. The result we have obtained seems only to cover the toe region of the stress strain curve. The stress-strain curves exhibit a bilinear nature with the initial slope of 1.82 MPa being nearly the same at all strain rates. At a strain rate of 259/s the slope of the second line is about 0.684 MPa, at the rate of 296/s the slope is 0.627 MPa and for the strain rate of 400/s the slope being 0.516 MPa. The aggregate slope after the knee region also appears to be the same with average value of 0.609 with about 15% variation. The difference between the loading curves seems to be driven by the transition point between the two slopes which seem to be larger for larger strain rates.

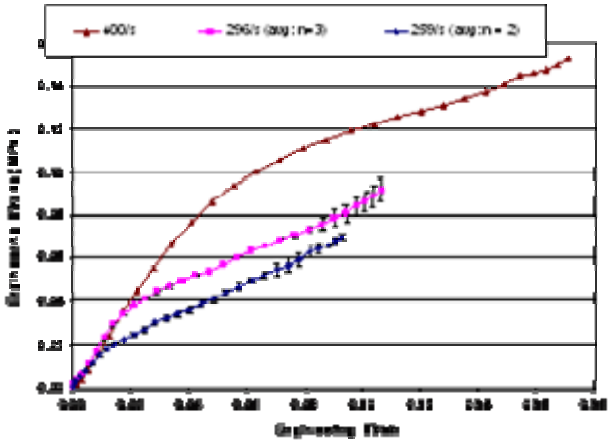

Fig. 10 Loading curve for human paraspinal erector spinae

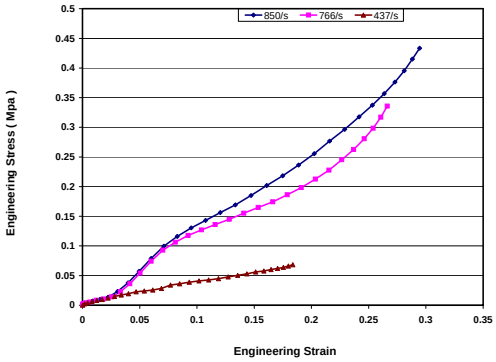

Fig. 11- Loading curve for human hamstring tissue at varying rates

Fig. 11 shows the variation of engineering stress to engineering strain for the hamstring muscles (H2) clustered at strain rates of 850/s (three samples), 766/s(two samples) and 437/s. As the thickness of the samples was less the thawing time required was around 10 minutes. The maximum engineering strain achieved for the strain rate of 850/s is 0.3 and the stress is 0.45 MPa. This data set can be classified as testing in the high strain rate zone for soft tissues and the stress range and strain ranges obtained were an order of magnitude higher than in H1 tests. The bilinear nature is not so prominent in this set. At strains above 0.1, the high strain rate curves exhibit a concave up shape, as has been reported in prior literature (Sligtenhorst et al., 2005)

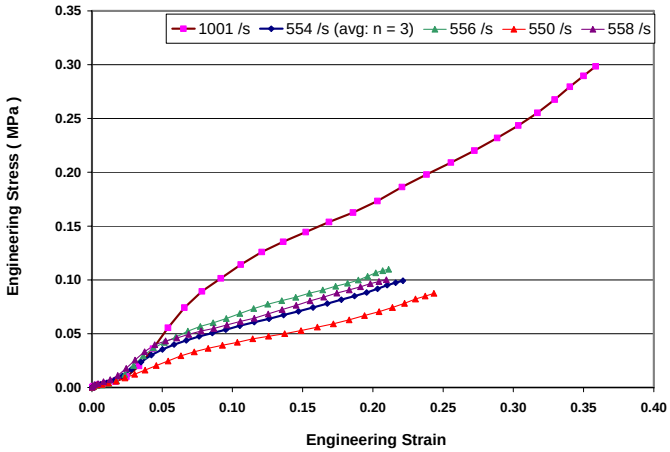

Fig. 12- **Loading curve for gluteus max at varying strain rates**

The third set was conducted to ascertain repeatability of the data. Three samples from gluteus max (H3) at a targeted rate of 550/s, yielded strain rates of 556/s, 550/s, and 558/s creating an average strain rate cluster of 554/s. The maximum engineering strain that was achieved with the setup for the strain rate of 554/s was 0.22 and the stress was 0.1 MPa. Fig. 12 shows the stress strain curves obtained at strain rates of 550/s, 556 /s and 558 /s and a mean curve computed at an average strain rate of 554/s. The slope between strains of 0.05 to 0.2 is 0.447 MPa with about 2% variation, demonstrating the test results are repeatable. Additionally one sample was tested at a strain rate of 1001/s. The behavior of this sample deviates significantly from the samples tested at lower strain rates.

To compare the behavior of different tissues, loading curves from the spine, hamstring and gluteus max tissue tested at similar strain rates have been plotted in Fig. 13 below. The behavior of the erector spine tissue is significantly different from the hamstring and gluteus maximus tissues. The elastic modulus is significantly higher for the spine tissue till the initial strain of 0.05. At strain magnitudes greater than 0.05, the tangent modulus is similar, though the stress magnitudes are different. The erector spine functionally resists flexion of the spine and is one of the strongest muscles in the body. The fascia layer covering it (dorsolumbar fascia) is also one the strongest tissues in the body. So there is a basis for the distinct behavior. However, since the samples are from different subjects and there is also some variation in the strain rates during measurement, a strong assertion cannot be made at this stage.

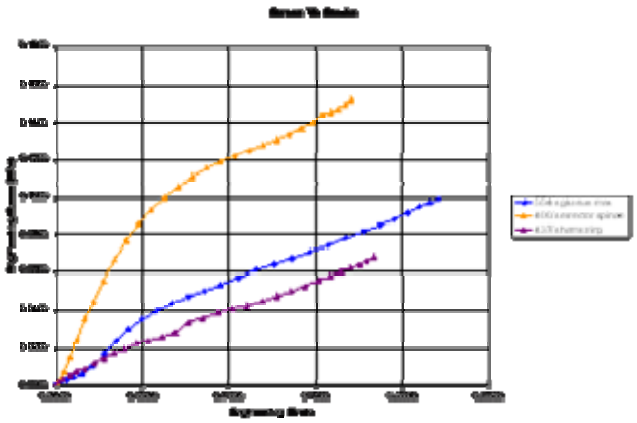

Fig. 13 Loading curves at similar strain rates for different tissues

CONCLUSION

An SHPB has been developed in order to test human body soft tissues at varying strain rates. A maximum strain of 0.3 was achieved with strain rates going up to 1000/s. Samples of the same tissue when tested at the same targeted strain rates produced reproducible results with less than 2% variation. Definite strain rate dependence of the loading curve is indicated. The loading curves exhibit multi linear behavior with increasing strain rate shifting the transition points between the slopes. Tissues from different muscles when tested at similar rates behave differently. At strain magnitudes greater than 0.05, the tangent modulus is similar for different tissues, though the stress magnitudes are different. The setup developed is small enough to be placed in the operation theaters so that testing can be conducted before properties change too much from in-vivo conditions. More extensive characterization and the development of a mathematical model to incorporate the effect of varying strain rates in the human body models used for crash modeling is planned.

REFERENCE

1. ASM Handbook, “Mechanical Testing and Evaluation”, Vol. 8, 1998, pp 425-560
2. Bacon, C. and Brun, A., 2000,“ Methodology for a Hopkinson test with a non-uniform Viscoelastic bar”, International Journal of Impact Engineering, Vol. 24, pp 219-230
3. Chen, W., Zhang, B., and Forestall, M. J., 1999, ‘‘A Split Hopkinson Bar Technique for Low-Impedance Materials’’, Experimental Mechanics, Vol. 39, pp. 81–85.
4. Cheng Z. Q., Crandall J. R. and Pilkey W. D., Wave dispersion and attenuation in viscoelastic spli hopkinson pressure bar, Shock and Vibration, Vol. 5, No. 5-6, 1998.
5. Graff, K.F., 1991, “Wave Motion in Elastic Solids”, Dover, New York.
6. Sawas, O., Brar, N. S., and Brockman, R. A., 1998, ‘‘Dynamic Characterization of Compliant Materials Using an All-Polymeric Split Hopkinson Bar’’, Experimental Mechanics, Vol. 38, pp. 204–210.
7. Sligtenhorst, C. V., Cronin D. S., and Brodland, G. W., “High strain rate compressive properties of bovine muscle tissue determined using a split Hopkinson bar apparatus, Journal of Biomechanics”, In Press.
8. Yunoshev, A. S. and Silvestre, V. V., 2001, “Development of the Polymeric Split Hopkinson Technique”, Journal of Applied Mechanics and Technical Physics, Vol. 42, No. 3, pp. 558-564.
9. Zhao, H., Gary, G., and Klepaczko, J. R., 1997, ‘‘On the Use of a Viscoelastic Split Hopkinson Pressure Bar’’, International. Journal of Impact Engineering, Vol. 19, pp. 319–330.

Back